OCEAN COLOR PRODUCTS RETRIEVAL AND VALIDATION AROUND CHINA COAST WITH MODIS

L. Sun [a], M. Guo [b], X. Wang [b]

[a] National Satellite Meteorological Center, China Meteorological Administration, No.46 South Avenue of Zhong-Guan-Cun, Beijing 100081, China - sunling@nsmc.cma.gov.cn

[b] National Satellite Ocean Application Service, National Oceanic Administration, No.8 Da-Hui-Si Road, Beijing 100081, China - (gmh,xmwang)@mail.nsoas.gov.cn

KEY WORDS: Atmosphere, Correction, Sea, Retrieval, Algorithms, Performance, Satellite, Optical

ABSTRACT:

Waters along China coast are very turbid with high concentrations of suspended sediment nearly all the time, especially at the Hangzhou Bay, the Yangtze River estuary and the shoal along Jiangsu province. In these turbid and optically complex waters, the standard MODIS ocean color products tend to have invalid values. Because the water-leaving radiances in the near-infrared (NIR) are significant resulting from the strong scattering of suspended particles, the standard MODIS atmospheric correction algorithm often gets no results or produces significant errors. And because of the complex water optical properties, the OC3 model used in the standard MODIS data processing tends to get extremely high chlorophyll-a (Chl-a) concentrations. In this paper, we present an atmospheric correction approach using MODIS short wave infrared (SWIR) bands based on the fact that water-leaving radiances are negligible in the SWIR region because of the extreme strong absorption of water even in turbid waters. A regional Chl-a concentration estimation model is also constructed for MODIS from in situ data. These algorithms are applied to MODIS Aqua data processing in the China coastal regions. In situ data collected in the Yellow Sea and the East China Sea in spring and autumn, 2003 are used to validate the performance. Reasonably good results have been obtained. It is noted that water-leaving reflectance in the NIR bands are significant in waters along the China coast with high sediment loadings. The satellite derived and in-situ reflectance spectra can match in the turbid waters along China coast, and there is relatively good linear relationship between satellite derived and in-situ reflectance. The RMSE value of $R_{rs}(\lambda)$ is 0.0031 for all the nine ocean color bands (412 to 869 nm). The satellite-derived Chl-a value is in the reasonable range and the root mean square relative error is 46.1%.

1. INTRUDUCTION

There are some of the most highly turbid coastal waters in the world along the China coastal region, especially in Hangzhou Bay, the Yangtze River estuary and the shoal along Jiangsu province, with consistently high concentrations of suspended sediment and complex optical properties. The performance of standard MODIS ocean color processing is poor in this region. There remain some issues related to the atmospheric correction and water constituent concentration estimation, e.g., chlorophyll a (Chl-a). The sensor-derived water-leaving radiances at the blue bands (e.g., 412 and 443 nm) are often biased low and sometimes even go negative, which often results from turbid waters with significant ocean radiance contributions at the near-infrared (NIR) bands (Siegel et al., 2000). The sensor-derived Chl-a concentration is often highly overestimated as the result of both biased water-leaving reflectance spectrum and estimation model not suitable for these complex waters.

In the standard MODIS atmospheric correction, black ocean assumption at the two NIR bands (748 and 869 nm) is adopted for the open ocean (Gordon and Wang, 1994; Gordon, 1997). However, due to the strong scattering of suspended particles, the water-leaving radiances in the NIR bands are significant for turbid waters. Based on the fact that water has much stronger absorption at the short wave infrared (SWIR) wavelengths than the NIR wavelengths, the water-leaving radiances are generally negligible at the SWIR bands even for very turbid ocean waters.

In the standard MODIS ocean color processing, the OC3 model is used for Chl-a concentration estimation (O´Reilly et al., 1998). However, due to the local features of ocean optical properties, this model is not proper for the turbid China coastal waters. Regional model should be constructed.

In this paper, an atmospheric correction algorithm using SWIR bands and a regional Chl-a estimation model are presented for MODIS. The ocean color products derived from MODIS Aqua data using these algorithms are reported and validated with in situ data collected in the Yellow Sea and the East China Sea.

2. RETRIEVAL ALGORITHMS

2.1 Atmospheric Correction Algorithm

For the ocean-atmosphere system, the top-of-atmosphere (TOA) reflectance measured by the satellite sensor in a spectral band centred at a wavelength λ, $\rho_t(\lambda)$, can be written as a linear sum of various contributions (angular dependencies are omitted):

$$\rho_t(\lambda) = [\rho_w(\lambda)+\rho_{wc}(\lambda)+\rho_g(\lambda)]T_g(\lambda)T_{r+a}(\lambda)+\rho_{atm}(\lambda) \quad (1)$$

$$\rho_{atm}(\lambda) = [\rho_{mix}(\lambda)-\rho_r(\lambda)]T_g(\lambda)+\rho_r(\lambda)T_g^{'}(\lambda) \quad (2)$$

where ρ_w = water-leaving reflectance
ρ_{wc} = whitecap reflectance
ρ_g = sun glint reflectance
T_g = gaseous absorption transmittance
$T_g^{'}$ = gaseous absorption transmittance excluding water vapour

T_{r+a} = scattering transmittance of the Rayleigh and aerosol mixing atmosphere
ρ_{atm} = intrinsic atmospheric reflectance reaching the sensor
ρ_{mix} = reflectance for the Rayleigh and aerosol mixing atmosphere not accounting for absorptive gases
ρ_r = reflectance for a pure Rayleigh atmosphere not accounting for absorptive gases

None water-leaving effects are calculated and removed from ρ_t to extract ρ_w. ρ_r is calculated using look-up tables with angles and surface pressure (Sun et al., 2006). T_g together with T_g' is calculated using formulas based on simulations with angles and gases amounts (Sun and Zhang, 2007). ρ_{wc} is estimated using an empirical model with wind speed (Koepke, 1984; Gordon, 1997). ρ_g is estimated using the Cox & Munk model with wind and angles (Cox and Munk, 1954). T_{r+a} is calculated using look-up tables with certain aerosol model, aerosol optical thickness τ_a and angles (Sun, 2005). To determine ρ_{mix}, mainly the aerosol contribution because ρ_r can be calculated in advance, $\tau_a \leftrightarrow \gamma$ ($\gamma=\rho_{mix}/\rho_r$) lookup tables with various aerosol models and angles are used (Sun and Guo, 2006; Antoine and Morel, 1999). Ten candidate aerosol models which are mainly based on four basic component mixing are adopted. The aerosol scattering phase function $P_a(\Theta)$ and normalized aerosol optical thickness $\Delta\tau_a$ are shown in Figure 1.

The water-leaving reflectance at two SWIR bands (centered at 1240 and 2130nm) are assumed zeros. Thus, $\gamma(1240)$ and $\gamma(2130)$ are obtained from ρ_t. $\tau_a(2130)_i$ for 10 aerosol models are calculated using $\tau_a \leftrightarrow \gamma$ lookup tables, and $\tau_a(\lambda)_i$ are extrapolated with the normalized optical thickness $\Delta\tau_a(\lambda)_i$, and $\gamma(1240)_i$ are reversely calculated using $\tau_a \leftrightarrow \gamma$ lookup tables. Then, two aerosol models (represented with *i*1 and *i*2) most similar to the actual one are selected according to $\gamma(1240)_{i1}<\gamma(1240)<\gamma(1240)_{i2}$, and the mixing ratio X for interpolation between two aerosols is calculated as $[\gamma(1240)-\gamma(1240)_{i1}]/[\gamma(1240)_{i2}-\gamma(1240)_{i1}]$. And then, for the visible and NIR bands, $\gamma(\lambda)_{i1}$ and $\gamma(\lambda)_{i2}$ are calculated from $\tau_a(\lambda)_{i1}$ and $\tau_a(\lambda)_{i2}$, and $\gamma(\lambda)$ is estimated as $(1-X)\gamma(\lambda)_{i1}+X\gamma(\lambda)_{i2}$, and $\rho_{mix}(\lambda)$ can then be calculated. Till now, ρ_w can be calculated from Equation (1).

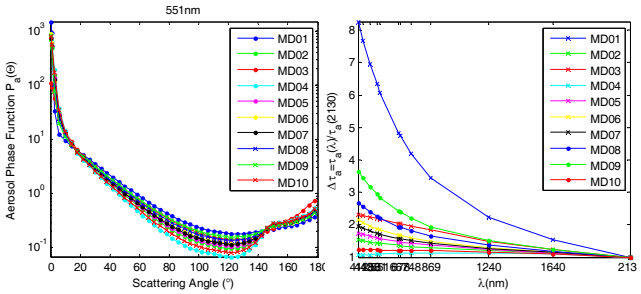

Figure 1. Aerosol scattering phase function for 551 nm band (a) and normalized aerosol optical thickness (b)

2.2 Chlorophyll-a Concentration Estimation Model

In situ chlorophyll-a concentrations were measured using HPLC method, and remote sensing reflectance spectra $R_{rs}(\lambda)$ from 350 to 1050 nm were derived from ASD measurements using above water method during the spring and fall of 2003 in the Yellow Sea and the East China Sea (Tang et al., 2004). Using the 76 data collected in fall (the maximum, minimum and mean Chl-a values are 35.9, 0.2 and 2.2 mg/m^3, respectively), an empirical model is constructed as follows:

$$\mathrm{Log}_{10}(\text{Chl-a}) = 0.118445 - 3.05761\mathrm{Log}_{10}(X_c) + 3.098626\mathrm{Log}_{10}^2(X_c) \quad (R^2=0.73) \tag{3}$$

$$X_c = [R_{rs}(443)/R_{rs}(551)][R_{rs}(412)/R_{rs}(488)]^{-0.8} \tag{4}$$

where R_{rs} = water remote sensing reflectance

The model has been tested with in situ R_{rs} data. The root mean square relative error is 45.3% for the 76 data used in model construction. When 83 data in spring (the maximum, minimum and mean Chl-a values are 15.2, 0.4 and 2.6 mg/m^3, respectively) are used for model testing, the root mean square relative error is 64.9%. Figure 2 provides the comparison between in situ Chl-a concentrations and model estimated Chl-a values from in situ R_{rs}. The results of linear fits for the data in fall and spring are also shown in the plot. The linear relationships between model estimated and in situ Chl-a are not very obvious with low correlation coefficient R^2.

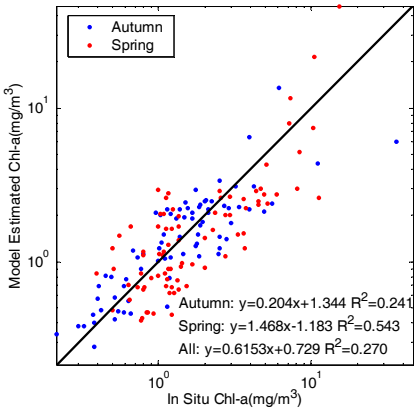

Figure 2. Model derived Chl-a values compared with in situ Chl-a concentrations

3. OCEAN COLOR PRODUCTS AROUND CHINA COAST

3.1 MODIS Ocean Color Products

MODIS Aqua data have been processed for the China coastal region using the SWIR atmospheric correction and Chl-a algorithm described in section 2. For the data processing, the MOD35 products have been used for cloud masking. Ancillary data including wind, ozone and water vapour are from climatology dataset. The derived products include water-leaving reflectance, chlorophyll-a concentration, and aerosol optical thickness (AOT), etc.

Figure 3a provides a MODIS Aqua true color image around the China coast on October 19, 2003. This image shows the very turbid waters along the China coast (brownish yellow to green in color), particularly the Hangzhou Bay, the Yangtze River estuary, and the shoal along Jiangsu province with extremely high sediment concentrations. Figures 3b-3h are examples of the de-

rived ocean color products corresponding to the MODIS data shown in Figure 3a. Figures 3b-3h are the images of water-leaving reflectance $\rho_w(\lambda)$ at wavelengths 443, 488, 551, 667 and 869 nm, chlorophyll-a concentration (Chl-a), and aerosol optical thickness at 869nm band $\tau_a(869)$, respectively. Values of $\rho_w(\lambda)$ from 443 to 667 nm bands (Figure 3b to 3e) are scaled linearly from 0.0 to 0.15, while $\rho_w(869)$ (Figure 3f) is scaled linearly from 0.0 to 0.05. Value of Chl-a (Figure 3g) is scaled logarithmically from 0.09 to 30 (mg/m3). Value of $\tau_a(869)$ (Figure 3h) is scaled from 0.0 to 0.6.

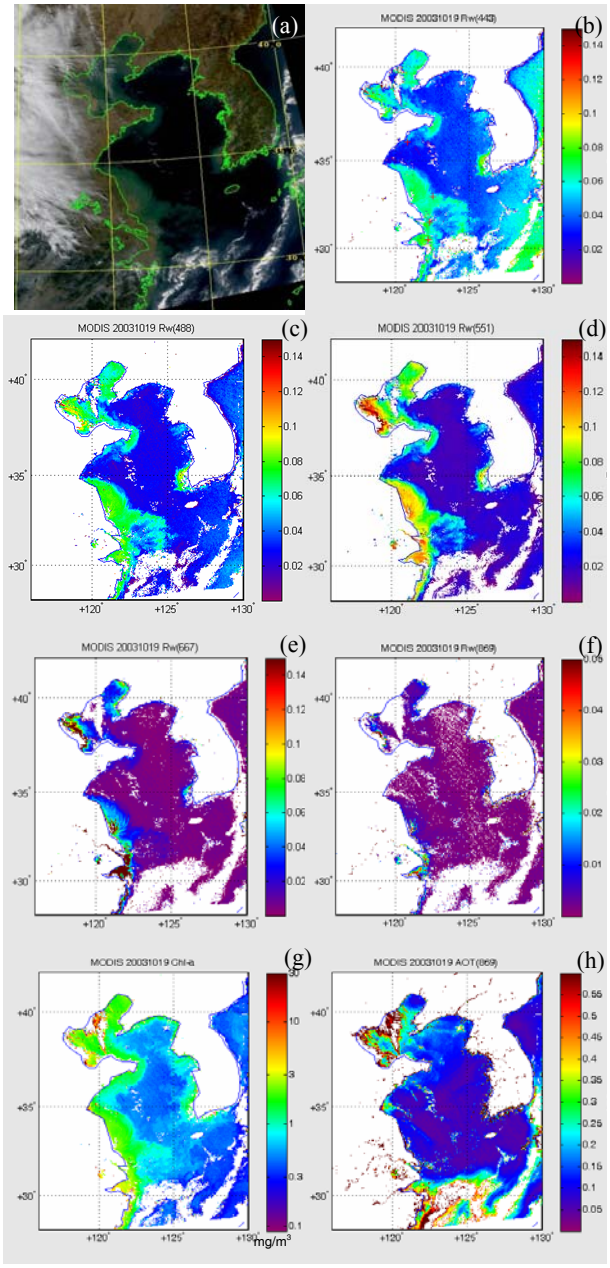

Figure 3. MODIS Aqua products on October 19, 2003 around the China coast for (a) true color image, (b-f) $\rho_w(\lambda)$ at 443, 488, 551, 667 and 869 nm bands, respectively, (g) Chl-a, and (h) $\tau_a(869)$

It can be seen that, along the China coastal region, the MODIS derived $\rho_w(\lambda)$ value increases from blue to green. The extremely high value in 667nm (Figure 3e) with brownish red color is due to the sensor saturation in this band. The NIR ocean contributions are significant, especially at the Hangzhou Bay, and some region in the Yangtze River estuary and the shoal along Jiangsu province. The MODIS-derived Chl-a values are in the reasonable range. And the results in Figure 3 show no obvious correlations between the derived oceanic properties ($\rho_w(\lambda)$ and Chl-a) and atmospheric property, e.g., $\tau_a(869)$.

3.2 MODIS Products Compared with In Situ Data

The remote sensing reflectance spectra $R_{rs}(\lambda)$ derived from in situ measurements during the spring and fall of 2003 in the Yellow Sea and the East China Sea are taken to be compared with those from MODIS-derived $\rho_w(\lambda)$ with the conversion of $R_{rs}(\lambda) = \rho_w(\lambda)/\pi$. Figure 4 provides four examples of these comparisons. The location in latitude and longitude and time difference between MODIS and in situ measurements are indicated in each plot. The in situ data were collected at the locations indicated in Figure 3b. The MODIS data were the average of pixels within ±0.015º centred at the in situ data location.

It shows in Figure 4 that the SWIR atmospheric correction performs reasonably well for these turbid waters. The in situ data shows high remote sensing reflectance values in NIR bands (748 and 869nm), i.e., the NIR $R_{rs}(\lambda)$ values range from 0.0006 to 0.003, while the values at site HD02 are relatively low. For these cases, the MODIS-derived $R_{rs}(\lambda)$ can match well with the in situ data except for site HD02 with underestimations at 667 to 748 nm bands.

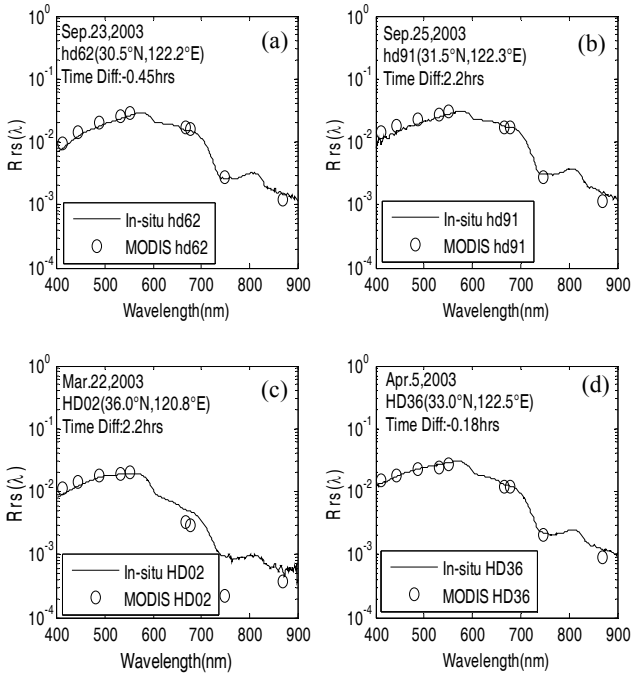

Figure 4. MODIS derived remote sensing reflectance spectra compared with those from in situ data acquired on (a) September 23, 2003, (b) September 25, 2003, (c) March 22, 2003, and (d) April 5, 2003

Figure 5 shows comparisons between the in situ and MODIS derived $R_{rs}(\lambda)$ values at the eight MODIS bands. In situ data

acquired within ±6 hours centred at the MODIS measurement time are included with a total of 20 match-ups. Although there are some noises, the results in Figure 5 show a relatively good linear relationship between MODIS and in situ $R_{rs}(\lambda)$. The slope of the linear fit for all the eight bands is 1.093, the intercept is 0.000702 and the correlation coefficient R^2 is 0.923. The results of linear fits for eight bands of 412, 443, 488, 531, 551, 667, 678, 748 and 869 nm are also shown in the plot, indicating more noise at the 412, 443 and 748 nm band. The MODIS derived $R_{rs}(\lambda)$ tends to be overestimated at 412 and 443 nm bands which may be subject to the radiative transfer precision and improper aerosol models. The RMSE values of $R_{rs}(\lambda)$ are 0.0054, 0.0054, 0.0032, 0.0029, 0.0036, 0.00095, 0.00094, 0.0010 and 0.0004 for 412, 443, 488, 531, 551, 667, 678, 748 and 869 nm bands, respectively. The RMSE for all dataset is 0.0031.

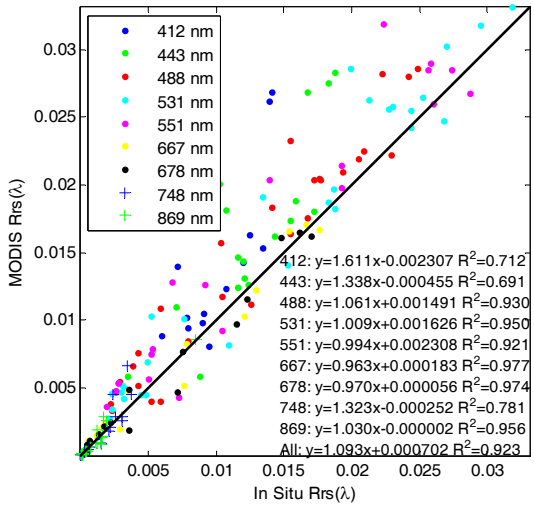

Figure 5. MODIS derived remote sensing reflectance values compared with in situ data for the bands of 412, 443, 488, 531, 551, 667, 678, 748 and 869 nm

The HPLC measured in situ chlorophyll-a concentration collected during the spring and fall of 2003 in the Yellow Sea and the East China Sea are taken to be compared with the MODIS-derived Chl-a. The root mean square relative errors are 45.5% and 47.1% for data in fall and spring, respectively. The root mean square relative error for all dataset is 46.1%. Figure 6 provides the comparison between the in situ and MODIS derived Chl-a values. The results of linear fits for the data in fall and spring are also shown in the plot. Similar with the result of model estimation from in situ R_{rs} shown in Figure 2, there is not a good linear relationship between MODIS derived and in situ Chl-a.

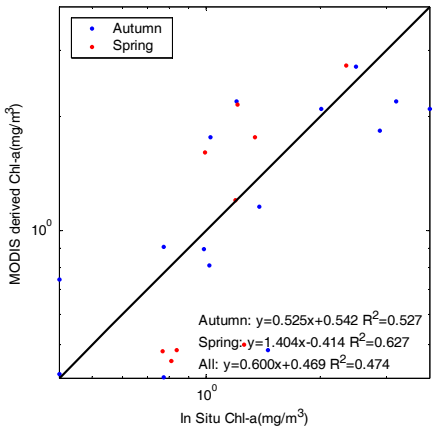

Figure 6. MODIS derived Chl-a values compared with in situ Chl-a concentrations

4. CONCLUSIONS

We have presented the SWIR atmospheric correction and Chl-a concentration estimation model for MODIS ocean color processing and used them to derive the MODIS Aqua water-leaving reflectance spectra and Chl-a along the China coastal region. In these turbid and optically complex waters, the standard MODIS ocean color products tend to have invalid values. By image analysis and comparing our MODIS derived ocean color products with those from in situ measurements collected in the Yellow Sea and the East China Sea, reasonably good results have been obtained. It is obvious that along the China coast with high sediment loadings, water-leaving reflectance in the NIR bands is significant. The satellite derived and in-situ reflectance spectra can match in the turbid waters along China coast, and there are relatively good linear relationship between satellite derived and in-situ reflectance in most of ocean color bands. The RMSE values of $R_{rs}(\lambda)$ are 0.0054, 0.0054, 0.0032, 0.0029, 0.0036, 0.00095, 0.00094, 0.0010 and 0.0004 for 412, 443, 488, 531, 551, 667, 678, 748 and 869 nm bands, respectively, and 0.0031 for all dataset. The satellite-derived Chl-a values are in the reasonable range and the root mean square relative error is 46.1%.

REFERENCES

Antoine, D., and Morel, A., 1999. A multiple scattering algorithm for atmospheric correction of remotely sensed ocean color (MERIS instrument): principle and implementation for atmospheres carrying various aerosols including absorbing ones. *Int. J. Remote Sens.*, 20(9), pp. 1875-1916.

Cox, C., and Munk, W., 1954. Measurements of the roughness of the sea surface from photographs of the Sun's glitter. *J. Opt. Soc. Am.*, 44(11), pp. 838-850.

Gordon, H. R., 1997. Atmospheric correction of ocean color imagery in the earth observing system era. *J. Geophys. Res.*, 102(D14), pp. 17081-17106.

Gordon, H. R., and Wang, M., 1994. Retrieval of water-leaving radiance and aerosol optical thickness over the oceans with SeaWiFS: a preliminary algorithm. *Appl. Opt.*, 33(3), pp. 443-452.

Koepke, P., 1984. Effective reflectance of oceanic whitecaps. *Appl. Opt.*, 23(11), pp. 1816-1824.

O'Reilly, J. E., Maritorena, S., and Mitchell, B. G., 1998. Ocean color chlorophyll algorithms for SeaWiFS. *J. Geophys. Res.,* 103(C11), pp. 24937-24953.

Siegel, D. A., Wang, M., and Maritorena, S., 2000. Atmospheric correction of satellite ocean color imagery: The black pixel assumption. *Appl. Opt.,* 39(21), pp. 3582-3591.

Sun, L., 2005. *Atmospheric Correction and Water Constituent Retrieval for HY-1A CCD*. PhD thesis, Institute of Oceanology, Chinese Academy of Science, Qingdao, China. (in Chinese)

Sun, L., and Guo, M., 2006. Atmospheric correction for HY-1A CCD in Case 1 waters. In: *Proceedings of SPIE, Remote Sensing of the Environment: 15th National Symposium on Remote Sensing of China*, Guiyang, China, Vol. 6200, pp. 20-31.

Sun, L., and Zhang, J., 2007. Analysis of influence of gaseous absorption on "HY-1A" CCD data: simulation and correction for Rayleigh scattering. *ACTA Oceanologica Sinica*, 29(3), pp. 137-145. (in Chinese)

Sun, L., Zhang, J., and Guo, M., 2006. Rayleigh lookup tables for HY-1A CCD data processing. *J. Remote Sens*, 10(3), pp. 306-311. (in Chinese)

Tang, J., Wang X., Song, Q., Li, T., Chen, J., Huang, H., and Ren, J., 2004. The statistic inversion algorithms of water constituents for Yellow Sea & East China Sea. *ACTA Oceanologica Sinica*, 23(4), pp. 617-626.

ACKNOWLEDGEMENTS

This research was supported by the National Natural Science Foundation of China (project 40606043) and National Basic Research Program of China (project 2006CB40370) and New-Tech Popularization Program of China Meteorological Administration (project CMATG2006Z02).